

SUPPLEMENTARY INFORMATION

Impact of the strength and spatial distribution of adsorption sites on methane deliverable capacity in nanoporous materials

Diego A. Gomez-Gualdron,^a Cory Simon,^b William Lassman,^a David Chen,^a Richard L. Martin,^{c,d} Maciej Haranczyk,^c Omar K. Farha,^{e,f} Berend Smit,^b Randall Q. Snurr.^{a}*

^a Department of Chemical and Biological Engineering, Northwestern University, 2145
Sheridan Road, Evanston, IL 60208, USA

^b Department of Chemical and Biomolecular Engineering, University of California,
Berkeley, Berkeley, CA 94709, USA

^c Computational Research Division Lawrence Berkeley National Laboratory, Berkeley,
CA 94720, USA

^d Watson Group, IBM Almaden Research Centre, San Jose, CA 95210, USA

^e Department of Chemistry, Northwestern University, 2145 Sheridan Road, Evanston, IL
60208, USA

^f Department of Chemistry, Faculty of Science, King Abdulaziz University, Jeddah 22254,
Saudi Arabia

I. SUPPLEMENTARY SIMULATION DETAILS

Here, we outline the methods to simulate the adsorption of methane in the model materials in scenarios 1 and 2. The computer codes used for these simulations are available online at <https://github.com/CorySimon/EmptyBox>. In both scenarios, we model methane as a Lennard-Jones sphere with parameters taken from the TraPPE force field.¹ That is, the energy of two methane molecules a distance r apart is modelled with a Lennard-Jones potential, $U_{gg}(r)$. We truncate our Lennard-Jones potential at radius of 12.8 \AA , which allows us to mimic a crystal of infinite extent by applying periodic boundary conditions.

$$U_{gg}(r) = \begin{cases} 4\epsilon \left(\left(\frac{\sigma}{r} \right)^{12} - \left(\frac{\sigma}{r} \right)^6 \right) & \text{if } r \leq 12.8 \text{ \AA} \\ 0 & \text{otherwise.} \end{cases} \quad (1)$$

For our grand-canonical Monte Carlo simulations, we convert the pressure of the bulk gas of methane into chemical potential using the Peng-Robinson equation of state <https://github.com/CorySimon/PREOS>.

Simulation details for scenario 1

For the model material in Scenario 1, we partition space into a set of voxels. The boundary of each voxel is a rhombic dodecahedral honeycomb; this honeycomb is the Voronoi diagram of an FCC lattice of points. Consequently, we define the Voronoi centers of the voxels as this FCC lattice. Each voxel can hold at most one methane molecule. The energy of an adsorbed methane molecule in a voxel is U_θ . We simulate the grand-canonical ensemble using a Monte Carlo algorithm under two cases. In the first case, adsorbed methane molecules do not interact with each other at all except through volume exclusion (one methane molecule per site). In the second case, we include interactions between the methane molecules by assigning energies of interaction. We will show that the former case is equivalent to the classic Langmuir adsorption model. The latter case resembles a mean-field approximation of a similar model, which results in the Temkin adsorption isotherm model, a perturbation on the Langmuir model.²

The model material in Scenario 1 is characterized by the background energy field U_0 and distance d between FCC lattice points, which are the Voronoi centers of the rhombic dodecahedral voxels.

Generating the lattice. Here, we outline how to construct an FCC lattice with distance d between points. We start with a primitive unit cell of the FCC lattice, a cube of dimension 1.414 Å with four points (see fcc.cssr). In this lattice, the points are a distance 1.0 Å apart. To construct a lattice with distance d between points, we simply scale the box length by d . To use the nearest image convention to apply periodic boundary conditions for computing methane-methane interactions, we must replicate this lattice until the cube is at least of length twice of the Lennard-Jones cutoff radius of 12.8 Å. For convenience, let $M = M(d)$ be the resulting number of voxels, even though d and U_0 are enough to completely characterize our rhombic dodecahedral honeycomb material.

Case with no methane-methane interactions. We now show that the grand-canonical ensemble in our model material results in a Langmuir isotherm when methane-methane interactions are neglected. Let V_0 be the volume of each voxel. The single-particle canonical partition function of an adsorbed methane molecule in a voxel is:

$$q = \Lambda^{-3} \int_{V_0} e^{-\beta U_0} dx = \Lambda^{-3} V_0 e^{-\beta U_0}. \quad (2)$$

As we integrate over the entire volume of the voxel, this model assumes that methane molecule is free to explore the entire space inside the voxel, where it experiences an energy U_0 .

The canonical partition function of N adsorbed molecules is then:

$$Q(N, M, T) = \binom{M}{N} q^N 1^{M-N}, \quad (3)$$

given that each adsorbed molecule is independent, an empty site has a partition function of unity, and there are $\binom{M}{N}$ ways to arrange N indistinguishable particles in the M voxels.

The grand-canonical partition function for our model material in equilibrium with a bath of methane with chemical potential μ is:

$$\Xi(\mu, M, T) = \sum_{n=0}^M Q(N, M, T) e^{\beta\mu N} = \sum_{n=0}^M \binom{M}{N} [qe^{\beta\mu}]^N \quad (4)$$

Using the binomial theorem:

$$\Xi(\mu, M, T) = (1 + qe^{\beta\mu})^M \quad (5)$$

We obtain the adsorption isotherm in our model material by computing the average particle number in the system of voxels:

$$\langle N \rangle = \frac{\partial \log \Xi}{\partial (\beta\mu)} = M \frac{qe^{\beta\mu}}{1 + qe^{\beta\mu}} \quad (6)$$

Using the definition of fugacity f , (units: pressure), this becomes the familiar Langmuir isotherm:

$$\langle N \rangle = M \frac{Kf}{1 + Kf}, \quad (7)$$

with the Langmuir constant related to our model material by

$$K = \beta V_0 e^{-\beta U_0} \quad (8)$$

Case with methane-methane interactions included. Here, the energy of an adsorbed methane molecule in voxel i is:

$$U_i = U_0 + \sum_{j \neq i} I(j) U_{gg}(r_{ij}) \quad (9)$$

where r_{ij} is the distance between the Voronoi centers of voxels i and j and $U_{gg}(r)$ is the truncated Lennard-Jones potential in [equation 1](#). The function $I(j)$ is an indicator function that is unity if voxel j is occupied and zero otherwise. Thus, in this model, the energy of interaction between two methane molecules in two different voxels is assigned by taking their positions as fixed at the Voronoi centers of the voxels. This is an approximation since [equation 2](#) presumes that each molecule freely explores the space inside a given voxel. We simulate the grand-canonical ensemble in our model material with the energy

prescription in [equation 9](#) since we could not find an analytical solution. Our two Monte Carlo trials for this model are: (1) attempt to add a particle (2) attempt to remove a particle. For (1), we choose a random lattice site. If the lattice site is occupied, we do nothing; if the lattice site is empty, we accept this Monte Carlo trial particle insertion with probability p_{add} . For (2), we choose a particle at random and accept the proposal to delete it with probability p_{remove} . Of course, if there are zero molecules in the system, we do not attempt a deletion. Next, we derive the acceptance probabilities p_{add} and p_{remove} using the Metropolis-Hastings algorithm.

We can characterize a microstate of our system by a vector x of dimension M ; entry i of x , x_i , is unity if voxel i is occupied and zero if it is empty. The probability of observing a particular microstate x with N particles ($\sum_i x_i = N$) in the grand-canonical ensemble (see [equation 4](#)) is:

$$p(x) = (V_0 e^{-\beta U(x)} \beta f)^{\sum_i x_i} \quad (10)$$

where $U(x)$ is the energy of the system with microstate x , which can be calculated by the energy prescription in [equation 9](#).

The probability of attempting to insert a particle in a given voxel is $\alpha(N \rightarrow N + 1) = \frac{1}{2} I/M$ since one of M voxels is chosen at random and we choose an insertion attempt with probability $\frac{1}{2}$. The probability of attempting to delete a given particle is $\alpha(N \rightarrow N - 1) = \frac{1}{2} I/N$ since we choose one of the N particles at random.

Consider a Monte Carlo trial move to add a particle, changing the current microstate x to a new microstate x' . Our constraint here is thus $\sum_i x_i = N$ and $\sum_i x'_i = N + 1$. For detailed balance, the Metropolis-Hastings algorithm enforces:

$$p_{add} = \min \left(1, \frac{\alpha(N + 1 \rightarrow N) p(x')}{\alpha(N \rightarrow N + 1) p(x)} \right) \quad (11)$$

From the above discussion,

$$\frac{\alpha(N + 1 \rightarrow N)}{\alpha(N \rightarrow N + 1)} = \frac{\frac{1}{2} \frac{1}{N+1}}{\frac{1}{2} \frac{1}{M}} = \frac{M}{N + 1} \quad (12)$$

and using [equation 10](#),

$$\frac{p(x')}{p(x)} = V_0 \beta f e^{-\beta(U(x)-U(x'))} \quad (13)$$

Thus, our acceptance probability for a particle addition is:

$$p_{add} = \min \left(1, \frac{V \beta f e^{-\beta(U(x)-U(x'))}}{N+1} \right) \quad (14)$$

where $V = V_0 M$ is the volume of the system

Using the same procedure for the particle deletion trial, going from microstate x to x'

$$p_{remove} = \min \left(1, \frac{N e^{\beta(U(x)-U(x'))}}{V \beta f} \right) \quad (15)$$

For these Monte Carlo trials, we need to calculate $U(x) - U(x')$, where x and x' differ only by one entry. Thus, we only need to calculate the energy of a particle in the particle voxel that we have randomly chosen for the insertion or deletion. We perform $750M$ Monte Carlo trials for each simulation and use $150M$ trials for equilibration (scaling it with the number of voxels, M).

Simulation details for scenario 2

Here, we simulate the grand-canonical ensemble in a volume V with a uniform, background energy U_0 . We simulate in a cubic volume of dimension twice the Lennard-Jones cutoff radius, 12.8 \AA , so that the nearest image convention can be applied for periodic boundary conditions.

The energy of particle i in the system is:

$$U_i = U_0 + \sum_{j \neq i} U_{gg}(r_{ij}) \quad (16)$$

where U_{gg} is the Lennard-Jones potential in [equation 1](#).

We perform grand-canonical Monte Carlo simulations, where the following three Monte Carlo trials are attempted each with probability $1/3$: (1) particle insertion, (2) particle deletion, (3) particle translation. For (1), a particle is inserted at a uniformly random position in the simulation volume. For (2), a particle is chosen at random for removal (if

there are no particles, we do nothing). For (3), we perturb each coordinate of a randomly chosen particle by a uniformly distributed number in $[-0.05, 0.05]$ Å.

The acceptance rules for this standard grand-canonical Monte Carlo simulation are in Ref. 3.

II. SUPPLEMENTARY FIGURES AND TABLES

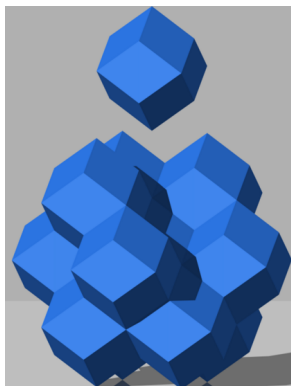


Figure S1. Rhombic dodecahedral honeycomb corresponding to the FCC-arranged methane pockets in scenario 1. One of the rhombic dodecahedral tiles corresponding to a methane pockets is separated and shown at the top.

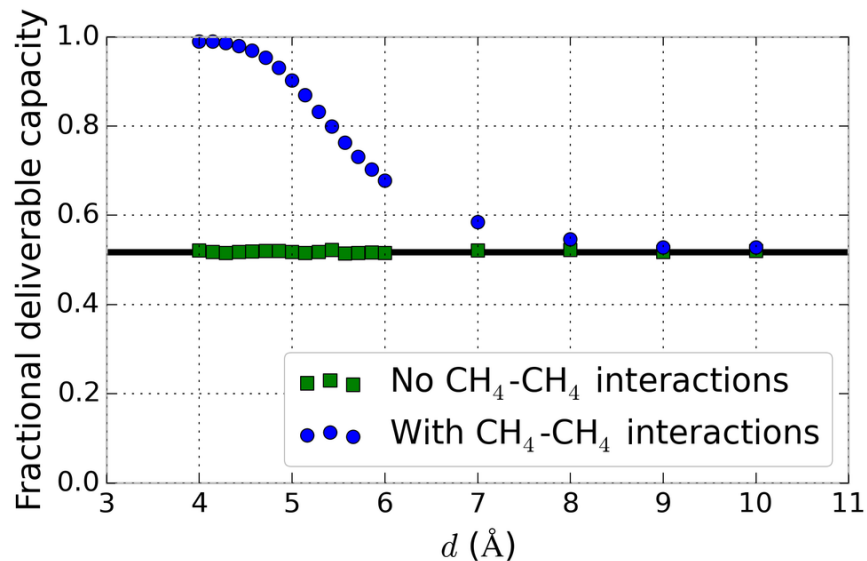


Figure S2. Maximum fractional deliverable capacity for each distance d in scenario 1 for the cases where methane-methane interactions are neglected (green points) and where methane-methane interactions are considered.

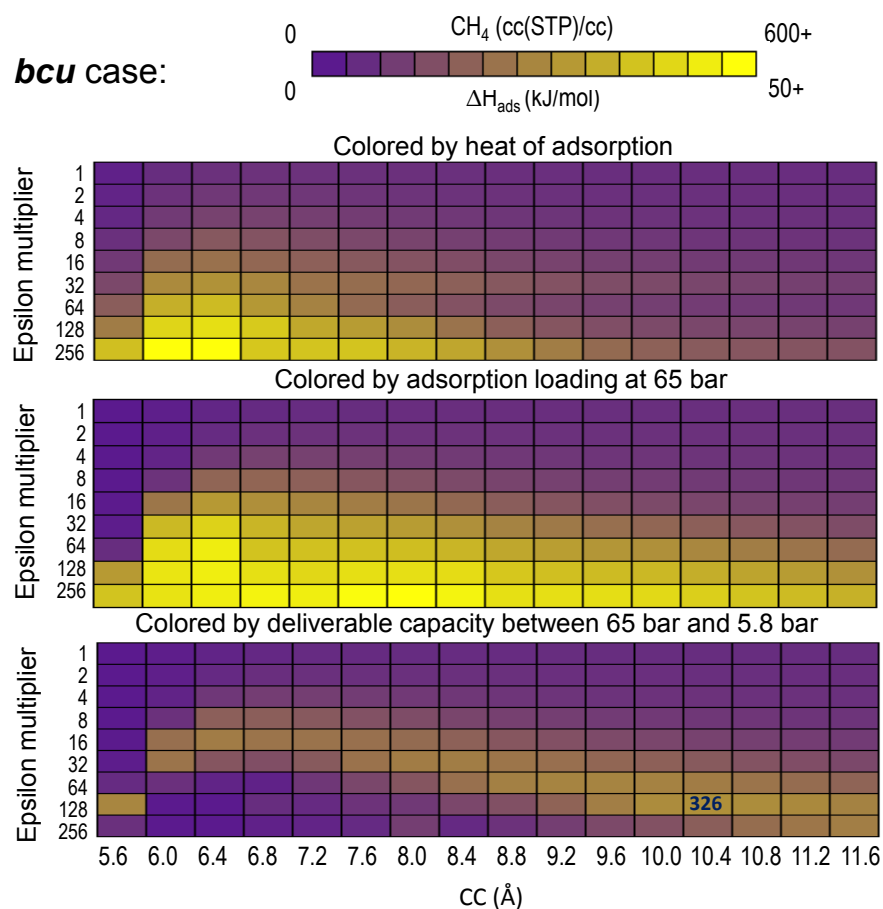


Figure S3 Data for the **bcu** case in scenario 3. In all panels, each “pixel” corresponds to a combination of epsilon multiplier and a distance between pseudoatoms *CC*. The color of the pixel indicates either methane heat of adsorption (top panel), methane loading at 65 bar (middle panel), or methane deliverable capacity between 65 and 5.8 bar (bottom panel) according to the top colored scale bar. The epsilon multiplier is in reference to the epsilon of carbon ($\epsilon_c = 52.8$ K). The highest deliverable capacity is annotated in the corresponding pixel.

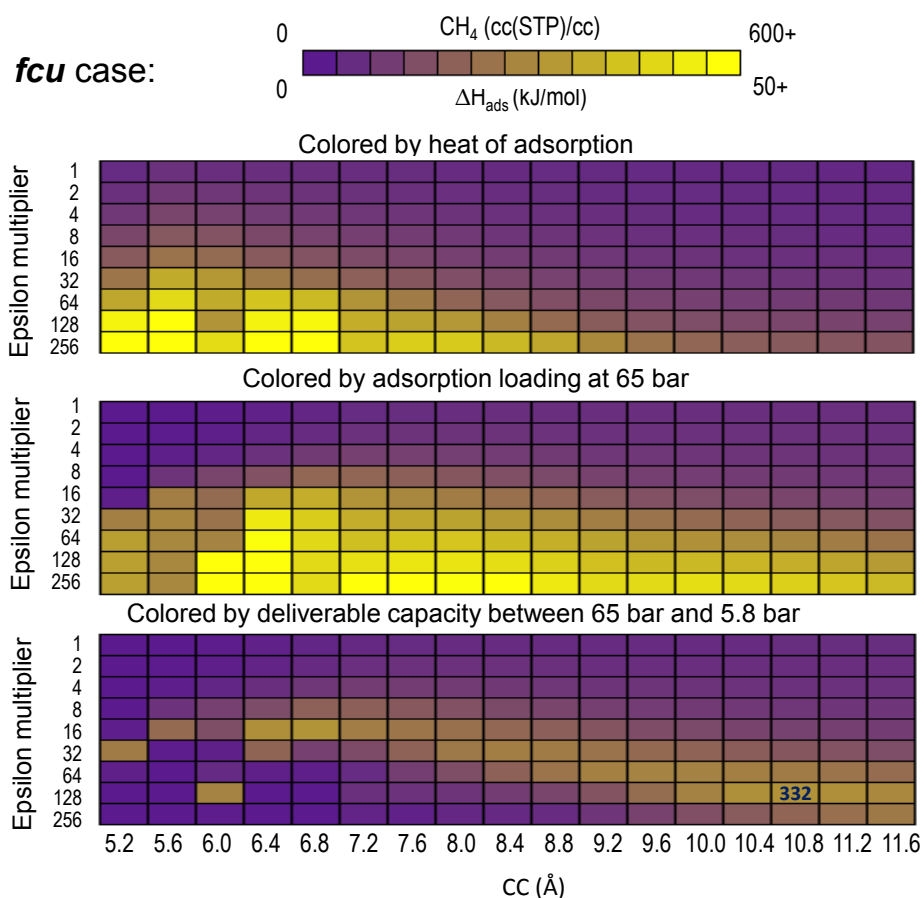


Figure S4 Data for the **fcu** case in scenario 3. In all panels, each “pixel” corresponds to a combination of epsilon multiplier and a distance between pseudoatoms CC . The color of the pixel indicates either methane heat of adsorption (top panel), methane loading at 65 bar (middle panel), or methane deliverable capacity between 65 and 5.8 bar (bottom panel) according to the top colored scale bar. The epsilon multiplier is in reference to the epsilon of carbon ($\epsilon_c = 52.8$ K). The highest deliverable capacity is annotated in the corresponding pixel.

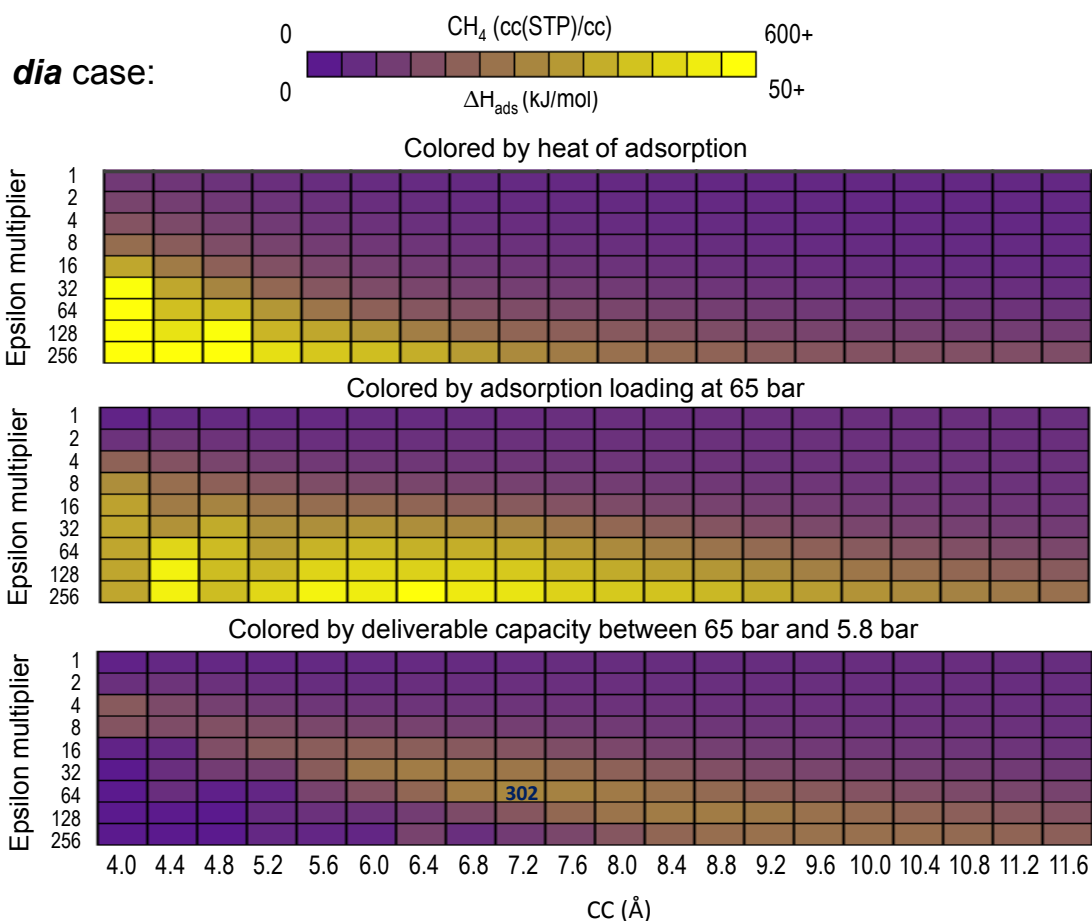


Figure S5 Data for the **dia** pseudoatom case in scenario 3. In all panels, each “pixel” corresponds to a combination of epsilon multiplier and a distance between pseudoatoms CC . The color of the pixel indicates either methane heat of adsorption (top panel), methane loading at 65 bar (middle panel), or methane deliverable capacity between 65 and 5.8 bar (bottom panel) according to the top colored scale bar. The epsilon multiplier is in reference to the epsilon of carbon ($\epsilon_c = 52.8$ K). The highest deliverable capacity is annotated in the corresponding pixel.

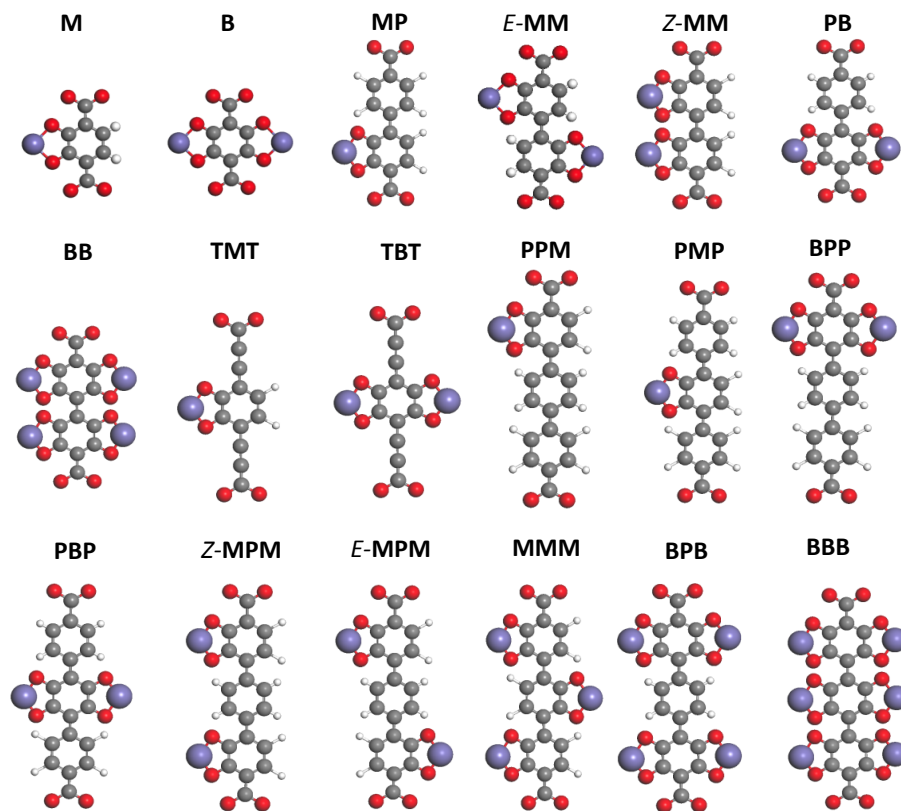


Figure S6. Linkers used to make derivatives of **pcu** and **fcu** parent MOFs. The letters denote the sequence of linker spacer groups. P: Phenyl; M: Monocatecholate; B: Bicatecholate; T: Ethynyl (triple bond).

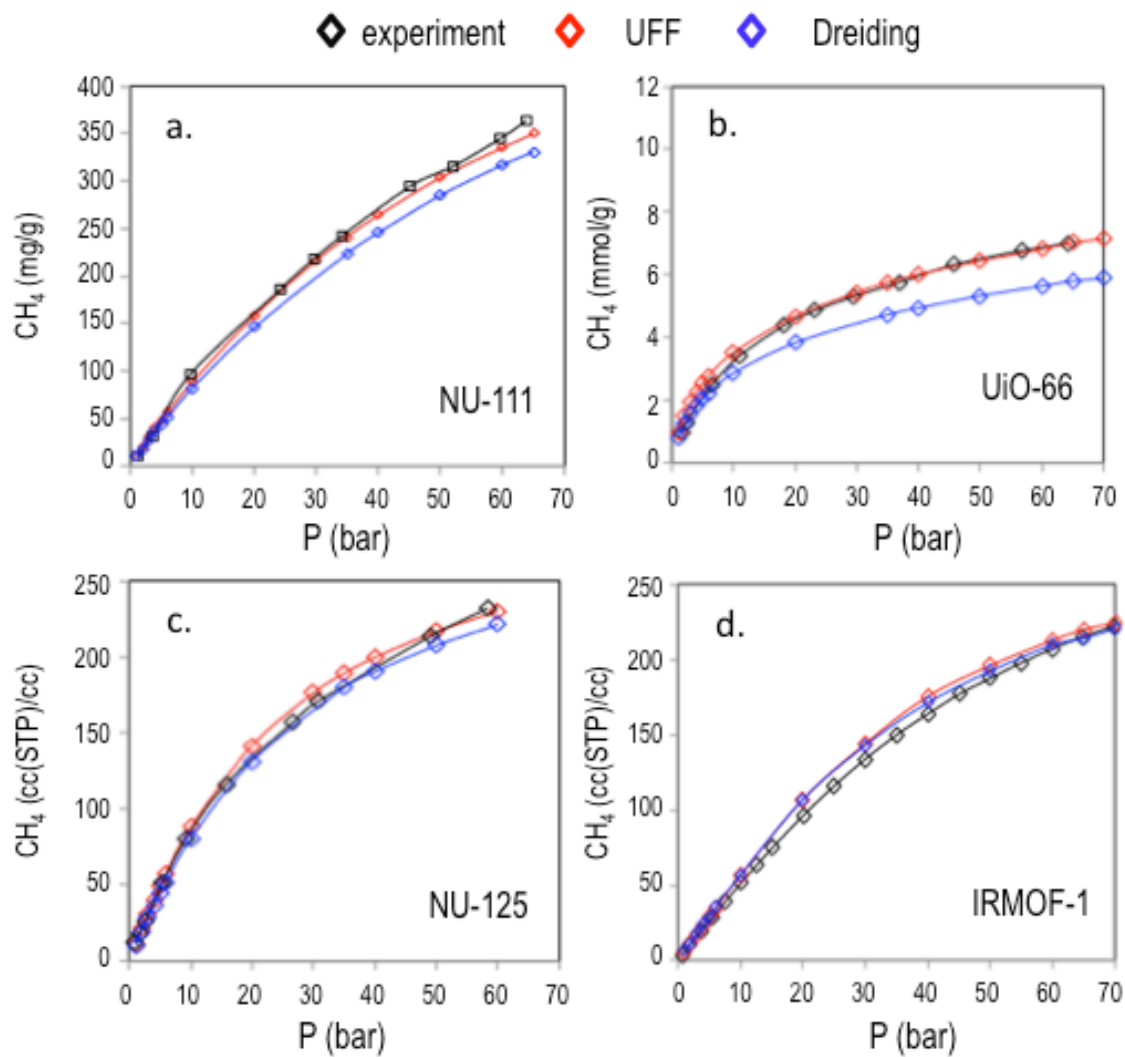


Figure S7. Comparison of experimental (black) and simulated (red and blue) isotherms calculated with Universal force field⁴ (red) and Dreiding force field⁵ (blue) for four well-known MOFs. **NU-111** (panel a) and **NU-125** (panel c) are based on the **rht** topology, whereas **UiO-66** (panel b) and **IRMOF-1** are based on the **fcu** and **pcu** topologies, respectively. Experimental data for NU-111 was obtained from ref. 6, for NU-125 from ref. 7, for UiO-66 from ref. 8 and for IRMOF-1 from ref. 9.

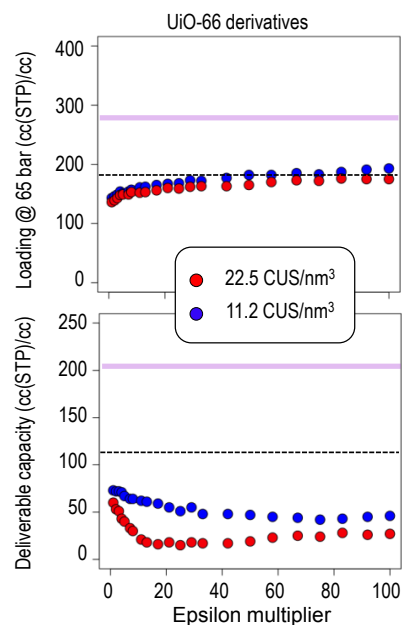


Figure S8. Methane loading at 65 bar (top) and deliverable capacity between 65 and 5.8 bar (bottom) versus the epsilon multiplier for the metal CUS for different derivatives of parent MOF **UiO-66**. The inset box relates the color of each curve and the respective CUS number density. The dashed lines represent the methane loading (top) or deliverable capacity (bottom) of the parent MOF. Solid lines represent the highest value of methane loading (top) or deliverable capacity (bottom) among the MOFs in [Figure 1](#).

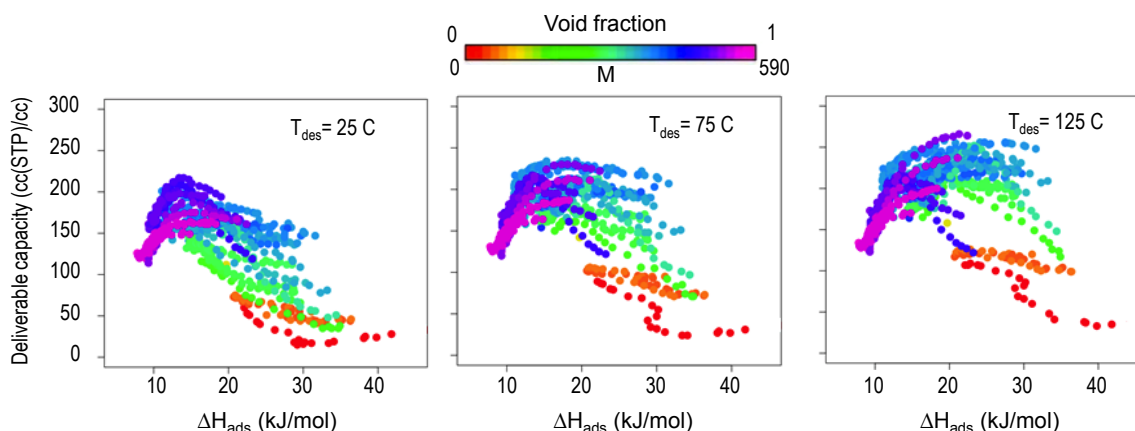


Figure S9. Deliverable capacity for all MOFs for which CUS were introduced via metalated catechol groups versus heat of adsorption (scenario 5) for three different desorption temperatures: 25°C (left panel), 75°C (center panel) and 125°C (right panel). Each point corresponds to a MOF, with the color indicating the void fraction of the structure according to the color scale at the top.

Table S1. Optimized geometries of functionalized benzene-methane complexes (side configuration). Distance “d” is the distance from the C atom of methane to the closest atom of the functional group.

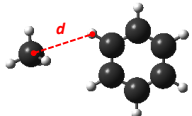
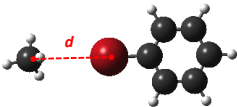
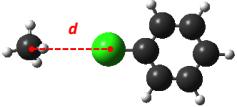
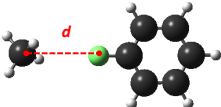
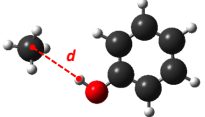
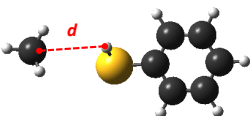
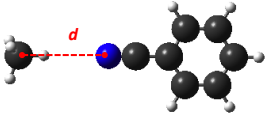
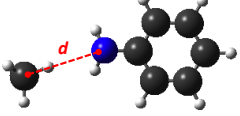
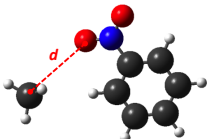
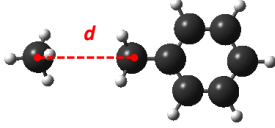
Geometry	Functional Group	Distance d (Å)	Multiplicity	Binding Energy (kJ/mol)
	H	3.0	1	-2.2
	Br	3.8	1	-1.5
	Cl	3.7	1	-1.1
	F	3.4	1	-0.5
	OH	2.7	1	-3.4
	SH	3.2	1	-1.7
	CN	3.9	1	-2.0
	NH ₂	3.7	1	-1.7
	NO ₂	3.6	1	-2.0
	CH ₃	2.5	1	-1.1

Table S2. Optimized geometries of functionalized benzene-methane complexes (top configuration). Distance “z” is the distance from the C atom of methane to the plane of the benzene ring.

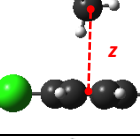
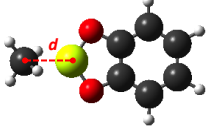
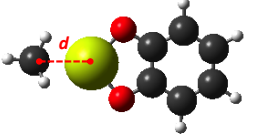
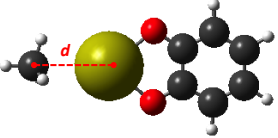
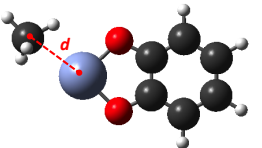
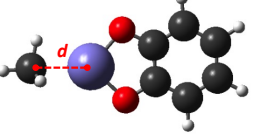
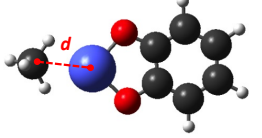
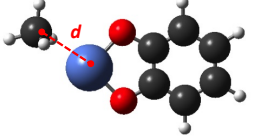
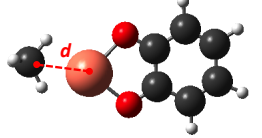
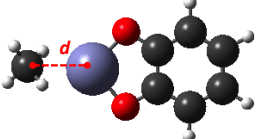
Geometry	Functional Group (FG)	Distance z (Å)	Multiplicity	Binding Energy (kJ/mol)
	H	3.6	1	-3.5
	Br	3.7	1	-4.5
	Cl	3.7	1	-3.3
	F	3.6	1	-3.8
	OH	3.5	1	-4.3
	SH	3.4	1	-4.5
	CN	3.4	1	-4.4
	NH ₂	3.6	1	-4.5
	NO ₂	3.3	1	-4.9
	CH ₃	3.5	1	-4.6

Table S3. Optimized geometries of metal catechol-methane complexes. Distance “d” is the distance from the C atom of methane to the metal atom.

Geometry	Metal	Distance d (Å)	Multiplicity	Binding Energy (kJ/mol)
	Be	2.0	1	-48.7
	Mg	2.4	1	-34.5
	Ca	3.0	1	-17.9
	Cr	2.5	5	-22.4
	Fe	2.3	5	-32.5
	Co	2.4	4	-22.4
	Ni	2.5	3	-31.9
	Cu	2.4	2	-12.4
	Zn	2.5	1	-23.8

REFERENCES

1. Martin, M. G.; Siepmann, J. I., *Transferable Potentials for Phase Equilibria. 1. United-Atom Description of n-Alkanes*, J. Phys. Chem. B **1998**, *102*, 2569-2577.
2. Simon, C. M.; Kim, J.; Lin, L.-C.; Martin, R. L.; Haranczyk, M.; Smit, B., *Optimizing Nanoporous Materials for Gas Storage*, Phys. Chem. Chem. Phys. **2014**, *16*, 5499-5513.
3. Smit, B. and Frenkel D., *Understanding Molecular Simulation: From Algorithms to Applications*, 2nd Edition, **2001**, Academic Press, London.
4. Rappe, A. K.; Casewit, C. J.; Colwell, K. S.; Goddard, W. A.; Skiff, W. M. *UFF, a Full Periodic Table Force Field for Molecular Mechanics and Molecular Dynamics Simulations* J. Am. Chem. Soc. **1992**, *114*, 10024-10035.
5. Mayo, S. L.; Olafson, B. D.; Goddard, W. A. *DREIDING: A Generic Force Field for Molecular Simulations* J. Phys. Chem. **1990**, *94*, 8897-8909
6. Peng, Y.; Srinivas, G.; Wilmer, C. E.; Eryazici, I.; Snurr, R. Q.; Hupp, J. T.; Yildirim, T.; Farha, O. K. *Simultaneously High Gravimetric and Volumetric Methane Uptake Characteristics of the Metal-Organic Framework NU-111* Chem. Commun. **2013**, *49*, 2992-2994.
7. Wilmer, C. E.; Farha, O. K.; Yildirim, T.; Eryazici, I.; Krungleviciute, V.; Sarjeant, A. A.; Snurr, R. Q.; Hupp, J. T. *Gram-Scale, High-Yield Synthesis of a Robust Metal-Organic Framework for Storing Methane and Other Gases* Energy. Environ. Sci. **2013**, *6*, 1158-1163.
8. Wu, H.; Chua, Y. S.; Krungleviciute, V.; Tyagi, M.; Chen, P.; Yildirim, T.; Zhou, W. *Unusual and Highly Tunable Missing-Linker Defects in Zirconium Metal–Organic Framework UiO-66 and Their Important Effects on Gas Adsorption* J. Am. Chem. Soc. **2013**, *135*, 10525-10532.
9. Mason, J. A.; Veenstra, M.; Long, J. R. *Evaluating Metal-Organic Frameworks for Natural Gas Storage* Chem. Sci. **2014**, *5*, 32-51